



## SEISMIC RELIABILITY OF BASE ISOLATED SYSTEMS WITH RUBBER BEARINGS

F. Micozzi <sup>(1)</sup>, F. Scozzese <sup>(2)</sup>, L. Ragni <sup>(3)</sup>, E. Tubaldi <sup>(4)</sup>, A. Dall'Asta <sup>(5)</sup>

- <sup>(1)</sup> *PhD Student, University of Camerino, fabio.micozzi@unicam.it*
- <sup>(2)</sup> *PostDoc, University of Camerino, fabrizio.scozzese@unicam.it*
- <sup>(3)</sup> *Associate Professor, Polytechnic University of Marche, laura.ragni@staff.univpm.it*
- <sup>(4)</sup> *Assistant Professor, University of Strathclyde, enrico.tubaldi@strath.ac.uk*
- <sup>(5)</sup> *Full Professor, University of Camerino, andrea.dallasta@unicam.it*

### **Abstract**

Seismically isolated systems are considered an effective solution to protect buildings and related content from earthquakes, and consequently reduce seismic losses. However, code conforming seismically isolated structures may have a seismic risk higher than expected target values. The reasons of this shortcoming are the lacks in the code prescriptions and for reliable design procedures and safety coefficients. The aim of the study is to investigate the seismic reliability of structural systems equipped with high-damping rubber bearings using a robust probabilistic framework in combination with advanced numerical models for the isolation system. In particular, the superstructure response has been simplified by using an uncoupled bidirectional elasto-plastic behaviour, while the nonlinear response of the rubber isolators has been simulated considering a fully 3D model accounting for the coupled behaviour in large displacements. The use of a simplified model for the superstructure allows to reduce the computational cost and to perform a parametric study by varying the design parameters of both the isolation system and the superstructure. For each varied design condition, the demand hazard curves expressing the mean annual rate of exceedance of a monitored response parameter, have been provided. The results show a strong effect of the design parameters on the reliability of the system and confirm that seismically isolated buildings designed by the minimum code requirements have a probability of failure higher than the codes prescription.

*Keywords: seismic isolation, rubber bearings, probabilistic analysis, structural reliability, Subset Simulation stochastic model*



## 1. Introduction

This paper focuses on seismic base isolation, which is an efficient and widely used technique for passive seismic protection of buildings and related content. This seismic solution is able to drastically reduce nonstructural damages even in the case of a severe earthquake, notably enhancing the resilience of buildings, thanks to the consequent reduction of the post-event recovery time. However, its ability to face exceptionally intense seismic events without disproportionate consequences (robustness) notably depends on the design criteria because base isolated structures are prone to brittle failure.

In particular, the system consists of two components, the isolation system and the superstructure, and the failure of one of them may cause the collapse of the building. Both these components may exhibit a brittle failure and the adequate choice of safety factors used in design is a key point to obtain a satisfactory safety level. Unfortunately, code prescriptions for isolator materials, fabrication or qualifications are often inadequate or even lacking [1]. Furthermore, prescriptions for displacement and strength capacity of bearing as well as for superstructure strength are not consolidated and are still matter of discussion and deeper investigations [1]. Differently, in the case of traditional steel or concrete structures, procedures to make high quality structural components are consolidated as well as safety coefficients to be used in the design. Moreover, they are based on redundant and ductile systems able to redistribute the structural damage, resulting in robust structures able to face exceptional events. As a result, while code conforming traditional solutions are characterized by adequate reliability levels, code conforming base-isolated structures may show reliability levels below the target suggested by the design codes. For example, American code [2] prescriptions for seismic design requires an “absolute” collapse probability lower than 1% in 50 years, as also illustrated and commented in [3]. In order to assess whether the probability of collapse of structures is under the target reliability level, risk analyses must be carried out by using probabilistic approaches. Recently, probabilistic risk analysis have been performed for base-isolated structures equipped with different kinds of isolators [1][4][5][6][7][8], as well as for structures equipped with dissipation devices, characterized by similar problems [9][10][11][12][13].

In this paper, an isolation system based on HDR (High Damping Rubber) bearings is considered. The aim is to investigate the seismic reliability of structural systems equipped with HDR bearings designed according to the European code on anti-seismic devices [14], which provides prescription for material, fabrication quality control and factory production tests of isolators, as well as some design recommendations. In particular, the study focuses on the influence of design rules in the system reliability and to this purpose a parametric analysis has been carried out by using a simplified tridimensional model. The model is composed of an uncoupled bidirectional elasto-plastic model describing the superstructure response, and a refined nonlinear model describing the tridimensional response of the rubber isolators and accounting for the coupling between vertical and horizontal response in large displacements [15][16][17]. The use of this simplified model reduces the computational effort required by advanced reliability analyses without a significant loss of accuracy in the results. This allows the development of a parametric study by varying the design parameters of both the isolation system and the superstructure. In particular, the varied parameters are the maximum shear deformation at the design condition, for what concerns the isolation system, and the response modification coefficient and the over-strength factor, for what concerns the superstructure. The influence of the above parameters on the seismic response of the system is evaluated by providing a comparison in terms of demand hazard curves for the two main engineering demand parameters: the maximum displacement of the superstructure and the maximum shear deformation of the isolation system. To this aim, a stochastic model is used for the seismic input and probabilistic analyses are performed via Subset Simulation, which is an efficient and robust tool useful for achieving accurate estimates of the risk up to very small failure probabilities.

## 2. Parametric analysis

### 2.1. Numerical model

Due to the high computational effort, a simplified model has been considered in this study to simulate the base-isolated structure. The model is based on the concept of the 2-DOF model originally proposed by



Kelly [18], where the superstructure is condensed in a single mass. Consequently, two masses  $m$  and  $m_b$  represent respectively the superstructure and the base mass, for a total mass of  $M = m + m_b$ . However, since a bidirectional input has been used in this study, the original model has been extended by using a bidirectional model for the superstructure and a full three-dimensional model for the isolation.

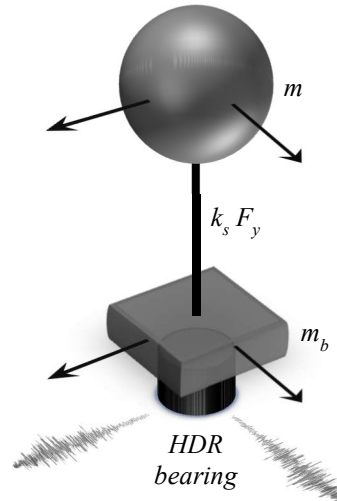


Fig. 1 – Isolation model

More in detail, the Kikuchi bearing element available in the Opensees software [19] has been used for the simulation of the mechanical behaviour of elastomeric bearings. It is a fully coupled tridimensional model, where the response is described by means of a two distribution of axial springs at the top and bottom ends of the element and a radial distribution of shear springs at the mid-height of the element [15]. The equilibrium equations of the element are written in the deformed configuration to take into account the coupling of the vertical and horizontal behavior, as originally proposed by Kelly [20]. In this study a single bearing has been modeled; consequently, the mass and the weight relevant to the bearing have been assigned to the simplified structural model. Considering a rigid diaphragm above the isolation level, the model is a good approximation of the real behavior of low-medium rise isolated building, where the superior modes take no role in the seismic response and the rocking effects are negligible. The superstructure has been modelled by two uncoupled elasto-plastic springs with stiffness  $k_s$  and yielding force  $F_y$ , describing the behaviour of the superstructure frame along the two main horizontal directions. A stiffness proportional damping is also provided to the superstructure.

The case study assumed in this paper is representative of low-medium rise buildings, where the superstructure has a fixed base period of 0,5s and a damping factor of 2%, typical of reinforced concrete structures equipped with seismic isolators [21]. In particular, considering a 4 floors building with 1 kNs<sup>2</sup>/m<sup>3</sup> distributed mass for each floor (5 floors including the base floor above the isolation system) with 2 x 4 spans of length of 5m (for a total of 15 columns and thus 15 bearings) the total mass of the building is 1000 kNs<sup>2</sup>/m. Consequently, the mass on a single bearing is 66.7 kNs<sup>2</sup>/m. The ratio between the condensed mass of the superstructure and the total mass of the system has been assumed equal to 0.6, which is a value representative of the described building. Then, the superstructure stiffness has been selected in order to obtain the target period of the superstructure with the assumed mass.

Finally, the dimension of the bearing and the yield force of the superstructure have been obtained by following the design procedure described in the next section. Different assumptions have been made in order to cover a range of real situations and in order to investigate the influence of the design choices on the seismic risk of base-isolated structures.



## 2.2. Design the base-isolated system

The isolation bearing has been designed in order to obtain an isolation period equal to  $T_{is}=3$  s. The design have been carried out using a set of 10 accelerograms representative of the seismic demand at the design rate of occurrence of  $2 \cdot 10^{-3}$ , typical of the Ultimate Limit State (ULS) of the Eurocode 8, as prescribed by the European standards [14][22]. For the parametric study three values of design shear deformation have been considered:  $\gamma_d=1$ ,  $\gamma_d=1.5$  and  $\gamma_d=2$ , lower than the limit of 2.5 imposed by the code on anti-seismic devices [14]. In particular, the height and the diameter of the isolation bearing ( $h_{is}$  and  $D_{is}$ ) have been determined iteratively in order to obtain a value of the average maximum shear strain as close as possible to the design one. For the bearing the rubber X0.4S has been used [23], whose equivalent linear parameters [14] are illustrated in Figure 2, as a function of the shear strain.

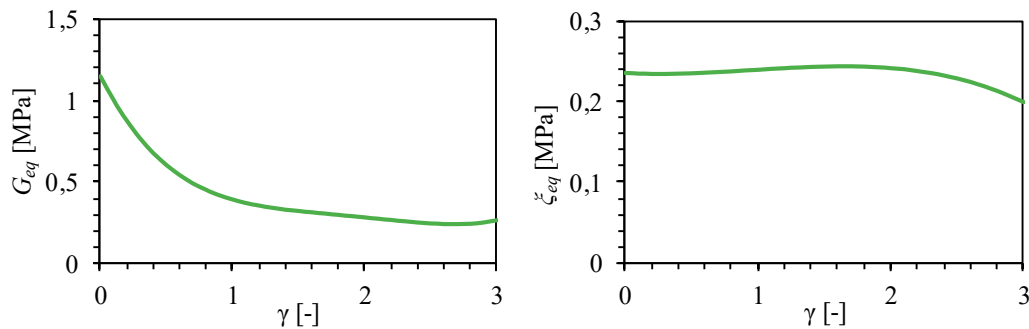


Fig.2 Equivalent linear parameters of the rubber X0.4S

Results of the design are summarized in Table 1, where the number and thickness of the single rubber layer are also reported. For completeness, also the compression stress is reported. All values are such that the stability verification is satisfied, according to the Eurocode on anti-seismic devices [14].

Table 1 – Dimensions of the isolation bearings

$\gamma_{is}$	$h_{is}$	$D_2$	$t_r$	$n$	$\sigma$
	[m]	[m]	[m]	[-]	MPa
1	0.196	0,431	0,0031	64	4.46
1.5	0.132	0,391	0,0028	47	5.45
2	0.097	0,357	0,0026	38	6.53

As already mentioned in the introduction, another important design parameter of isolated buildings is the superstructure strength, which depends on the seismic demand at the design condition, i.e. the total force acting on the superstructure (or superstructure base shear). The Eurocode [22] allows to reduce the design value of the base shear by a behaviour factor  $q$  in the range [1, 1.5]. The two extreme cases have been considered in the parametric analysis. Furthermore, it is expected that the actual elastic limit of the structure is larger than the design value. This is due to safety factors applied to material strengths and structure redundancy. Usually, the over-strength ratio  $\Omega$ , expressing the ratio between the actual elastic limit and the design strength, is approximately equal to 1.5 [24]. Non-structural elements may also notably contribute to increase the elastic limit, especially in the case of strong infill panels, and the over-strength factor may grows up to value of 2.5 [7]. The two parameters (behaviour factor  $q$  and over-strength ratio  $\Omega$ ) can be combined in the ratio  $\Omega/q$  to express directly the ratio between the actual strength capacity and the seismic demand of the superstructure. Table 2 shows all the case studies analysed with the different values of the ratio  $\Omega/q$  assumed in the parametric analysis, considering different combination of  $q$  [1,1.5] and  $\Omega$  [1.5,2.5]. The yield force of the superstructure model obtained by applying the design procedure is also reported for each analysis case.



Table 2 – Superstructure parameters for the analyzed cases

$\gamma_{ts}$	$\Omega/q$	$F_y$
[-]	[-]	[kN]
2	1	38
1,5	1	36
1	1	33
2	1.5	57
1,5	1.5	54
1	1.5	49
2	2.5	95
1,5	2.5	90
1	2.5	82

### 3. Probabilistic approach

#### 3.1 Demand hazard curves

This section describes the tool used to estimate the demand hazard curves for the main response parameters of isolated systems, describing the mean annual frequency (MAF) of exceedance of the considered parameter according to the selected hazard. In particular, the evaluation of the demand hazard according to the unconditional approach can be formalized as follows:

$$\nu_D(d) = \bar{\nu} G_D(d) \quad (1)$$

where  $\bar{\nu}$  denotes the MAF of occurrence of at least one event within the range of intensity levels of interest, which is a function of the recurrence law for the seismic source, and  $G_D(d) = P[D > d]$  is the probability of exceedance of the demand  $d$ , given the occurrence of an earthquake of any intensity.

Obviously, in order to generate a demand hazard curve,  $\nu_D(d)$  must be estimated for different values of the demand, up to very low exceedance probabilities. In this study, the demand hazard curves are estimated via Subset Simulation [25]. The basic idea behind this advanced simulation technique is to express the rare-event probability  $G_D(d_l)$  in terms of the product of larger conditional probabilities, by introducing intermediate exceedance events corresponding to lower threshold values  $d_1 < d_2 < \dots < d_l$ . In the analyses, the original implementation [25][26] of the method is employed. This relies on the Markov Chain Monte Carlo algorithm and the Metropolis–Hastings sampler to efficiently and adaptively generate samples conditional on the intermediate failure regions and thus gradually populate from the frequent to rare event region. Assuming a fixed value  $p_0$  for the conditional probabilities of exceedance of the various thresholds, each time a set of  $n_{sim}$  samples is generated through the Metropolis–Hastings algorithm (standard Monte Carlo simulation for the first threshold), and the corresponding demand threshold  $d_i$  is simply evaluated as the  $(1-p_0)n_{sim}$ -th largest value. The exceedance probability of the  $i$ -th threshold, computed by carrying out  $i$ -times the product of the same probability  $p_0$ , is  $p_0^i$ , for  $i=1, 2, \dots, l$ , and the lowest obtained value of the failure probability is  $p_0^l$ .

The results obtained by Subset Simulation are practically unbiased and on average they converge to the reference results furnished by the robust direct Monte Carlo simulation.

#### 3.2 Seismic hazard and stochastic ground motion model

The adopted seismic hazard is representative of an Italian high seismicity zone. Similarly to [27][28][29] the seismic scenario is described by a source model characterized by two main random seismological



parameters, namely the moment magnitude  $M$ , and the epicentral distance  $R$ . A Gutenberg-Richter recurrence law [30] is used to describe the magnitude-frequency relationship of the seismic source:

$$v_M(m) = 10^{(a-bm)} \quad (2)$$

in which the parameter  $a$  accounts for the mean number of earthquakes expected from the seismic source, while the parameter  $b$  is a regional seismicity factor governing the proportion of small to large earthquakes. The assumed recurrence law, bounded within the range of magnitudes of interest  $[m_0, m_{max}]$ , leads to the following probability density function (PDF) of the moment magnitude [29][30]:

$$f_M(m) = \beta \frac{e^{-\beta(m-m_0)}}{1 - e^{-\beta(m_{max}-m_0)}} \quad (3)$$

being  $\beta = b * \log_e(10)$ ,  $m_0$  the magnitude value below which non-significant effects are expected on the structures, and  $m_{max}$  the physical upper bound of the magnitudes expected from the source. In this application, it is assumed  $m_0 = 6$ ,  $m_{max} = 8$ ,  $a = 3.5$  and  $b=0.8$ . The epicentral distance is modelled according to the following PDF:

$$f_R(r) = \begin{cases} \frac{2r}{r_{max}} & \text{if } r < r_{max} \\ 0 & \text{otherwise} \end{cases} \quad (4)$$

which is obtained under the hypothesis that the source produces random earthquakes with equal likelihood anywhere within a distance from the site  $r_{max} = 70$  km, beyond which the seismic effects are assumed to become negligible. The soil condition is described by a deterministic value of the shear-wave velocity parameter  $V_{S30} = 255$  m/s, representative of deformable soil condition [31].

The Atkinson-Silva [32] source-based ground motion model is used to describe the attenuation from the source to the building site. This model, combined with the stochastic point source simulation method of [33], is employed to generate ground motion samples conditional to the samples of  $M, R$ . Fig. illustrates the ground motion total radiation spectrum  $A(\omega)$  (i.e., the Fourier spectrum), and the time-envelope function  $e(t)$ , obtained for different earthquake moment magnitudes  $m$  (5, 6.5, 8) and a fixed epicentral distance  $r=20$  km.

For the simulation of two horizontal ground motion components, the stochastic model is modified as suggested by [34], according to which the radiation spectra can be considered to have the same shape for the two horizontal orthogonal directions, but the intensities are scaled by two different scaling random parameters (random scaling disturbance  $\varepsilon_1, \varepsilon_2$ ) generated as samples of a multivariate lognormal distribution with zero mean, standard deviation  $\sigma = 0.523$  (similarly to what suggested by [27] for unidirectional seismic actions) and correlation  $\rho = 0.8$  [35]. This way, the target radiation spectra along directions 1 and 2 will be equal to  $A_1(\omega)=\varepsilon_1 A(\omega)$  and  $A_2(\omega)=\varepsilon_2 A(\omega)$ .

The random scaling disturbance ( $\varepsilon_1, \varepsilon_2$ ), together with the Gaussian white noise process ensure the ground motions record-to-record variability to be accounted for. In particular, for each earthquake sample a Gaussian white noise signal is generated and, after being windowed through the envelope-functions  $e(t)$  (Fig. b), its normalized frequency spectrum is applied to the target radiation spectrum (Fig. a), thus providing the variability of the energy content within the frequency domain. Such variability is further amplified by the lognormally-distributed multiplicative factors ( $\varepsilon_1, \varepsilon_2$ ) of the radiation spectra. The resulting overall variability provided by the model is shown in Fig. a, in which the spectra of three earthquake samples corresponding to the same pair of magnitude and distance (i.e.,  $m = 7$  and  $r = 20$  km) are depicted in different colours. It can be observed how the Fourier spectral amplitudes differ sample-by-sample, with peaks randomly distributed over the frequencies, although on average the trends are fully defined once the input parameters are fixed ( $M, R, V_{S30}, \varepsilon_1, \varepsilon_2$ ). For the sake of completeness, the acceleration time series corresponding to the three aforesaid spectra are also plotted in Fig. b.

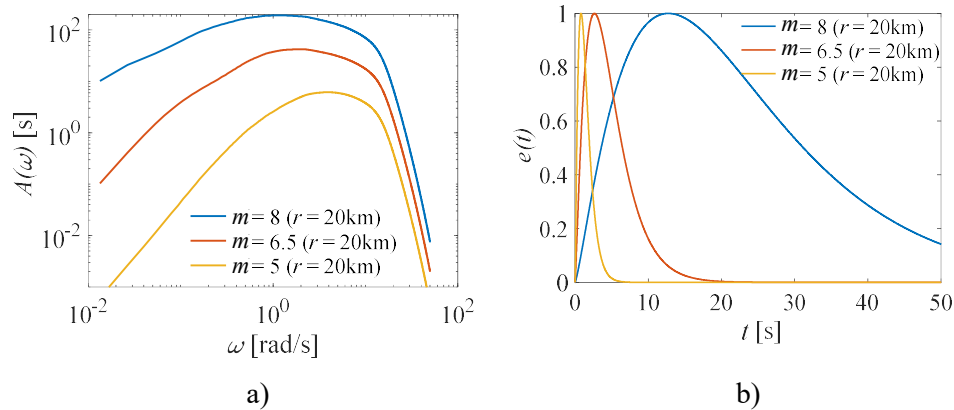


Fig. 3 a) Radiation Fourier spectra and b) time-envelope functions for  $r = 20$ km and different  $M$  values.

Source: Scozzese et al. (2019) [10]

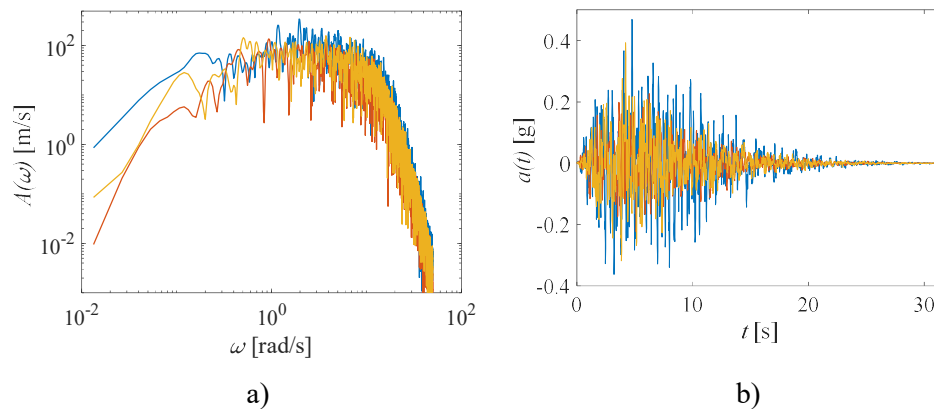


Fig. 4 a) Radiation Fourier spectra and b) acceleration time series for 3 simulations with  $m = 7$  and  $r = 20$  km.

Source: Scozzese et al. (2019) [10]

### 3. Results of the probabilistic analysis

Fig. 5 illustrates results of the probabilistic analysis carried out on the simplified structural systems representing base-isolated bindings designed by assuming different design choices, as previously illustrated. Results are in terms of demand hazard curves of the monitored response parameters, expressing quantitatively the reliability of the isolated building, i.e. the MAF of exceedance of the response parameters. In particular, demand hazard curves in terms of maximum bearing shear strain  $\gamma_{iso}$  in any direction are reported on the left side of Fig.5 (a,c,e) for the different design situations, whereas on the right side (b,d,f) results refer to the maximum relative displacement in the x or y direction of the superstructure  $u_s$ , according to the decoupled model of the superstructure.

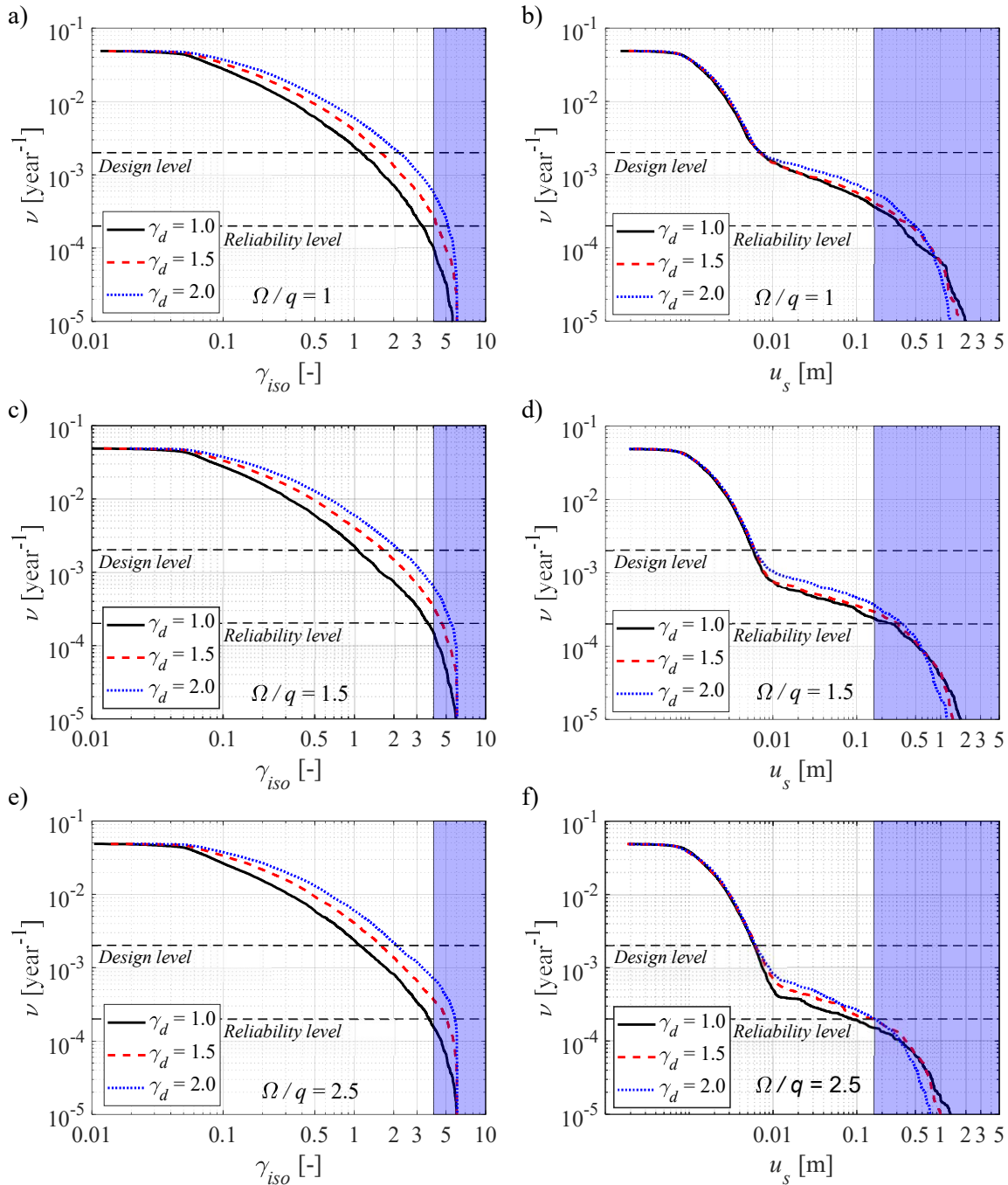


Fig. 5. Demand hazard curves of  $\gamma_{iso}$  and  $u_s$  for different  $\gamma_d$  and  $\Omega/q$  design values

The first remark refers to the bearing shear strain at the design hazard level corresponding to a MAF of  $2 \cdot 10^{-3}$  (dotted horizontal line). As expected, all the curves of  $\gamma_{iso}$  (Fig.5 a,c,e) intercept the design MAF close to the corresponding design shear deformations ( $\gamma_d=1$ ,  $\gamma_d=1.5$  and  $\gamma_d=2$  for the three cases analyzed). A limit of shear strain of 4 is highlighted in the figures, representing both the limit of the numerical model employed but also a limit for shear strain capacity of HDR bearings, according to the available literature [8][36][37]. It is evident that only in the case of  $\gamma_d=1$  (black curves) is possible to achieve the reliability level corresponding to 1% of probability of failure in 50 years, i.e. a MAF of  $2 \cdot 10^{-4}$ , which is the maximum level permitted by seismic codes [2][3]. The ratio between shear strain value at the target MAF and the value assumed in the design is the minimum safety factor to be applied in order to ensure the target reliability. For the case of  $\gamma_d=1$





and  $\Omega/q=1$  (Fig. 5a) this safety factor is about 3.5. Slightly larger values are obtained for the cases with  $\Omega/q=1.5$  (Fig. 5c) and  $\Omega/q=2.5$  (Fig.5e), showing a reduced but not negligible influence of this parameters on the isolation displacements. It is important to highlight that all these values are significantly larger than the amplification coefficient suggested by the European code on anti-seismic devices [14] to check the horizontal displacement capacity of the bearings. In fact, the code prescription is to carry out a ramp test up to a displacement equal to the design displacement amplified by two factors: a magnification factor  $\gamma_x$  aimed at increasing the reliability of the structural system and a further partial factor  $\gamma_b$ . For elastomeric bearings used in base-isolated buildings these factors are 1.2 and 1.15, whose product is significantly lower than value obtained from the risk analysis. As also observed by other authors [1], smaller amplification factors would be obtained by assuming a design seismic hazard with a smaller MAF [2][39].

The hazard curves of the superstructure relative displacement are illustrated in Fig. 5b,d,f for the different values considered of the ratio  $\Omega/q$ . The limit highlighted in the figures corresponds to a superstructure relative displacement of 0.16m, i.e. an average inter-storey drift of 2% of the story height for the considered case study building. It is noted that, increasing the over-strength ratio the yielding of the superstructure (identified by the bending point in the curve) moves closer to the reliability target. Anyway, the MAF of the superstructure yielding is always higher than the reliability target. After yielding all the hazard curves strongly change the slope and a little change in the MAF strongly increase the deformation demand of the superstructure. However, this demand decreases as the ratio  $\Omega/q$  increases and becomes feasible in the last case with  $\Omega/q=2.5$ . Only in this case the superstructure relative displacement does not exceed 0.16m which guarantees the absence of collapse for a low-ductility superstructure. These results confirm that the ductility demand of isolated structure can very high [40], especially in the case of a limited over-strength. Finally, it can be also observed that also in this case the design shear strain of the isolation system has a smaller influence on the superstructure displacement, even if not negligible.

## 5. Conclusions

In this study the seismic reliability of structural systems isolated with high-damping rubber bearings has been investigated, using a robust probabilistic framework in combination with advanced numerical models for the isolation system. In particular, the superstructure response has been simplified by using an uncoupled bidirectional elasto-plastic behaviour, while the nonlinear response of the rubber isolators has been simulated considering a fully 3D model accounting for the coupled behaviour in large displacements. A parametric study has been carried out by varying the design parameters of both the isolation system and the superstructure. For each variated design condition, the demand hazard curves have been provided expressing the mean annual rate of exceedance of a monitored response parameter. The results show that, for the hazard selected in this work, the probability of failure prescribed by the codes is attained only if the design shear strain of the bearings is much lower than displacement capacity. Then, during the design phase a safety factor significantly higher than the one defined by the code should be applied to the displacement capacity in order to obtain the design shear strain value or, alternatively, a larger hazard should be used as design action. Another interesting result is that the superstructure can achieve the target reliability level only in the case with the largest over-strength and that, even in this case, after the yielding a ductility capacity is required to the superstructure. However, these results should be confirmed by using a more advanced model of the superstructure. Furthermore, the obtained results for both the structural system components (isolation system and superstructure) are strongly related to the characteristics of the hazard selected for the analyses, thus different input should be accounted for in order to obtain more general conclusions.



## 6. References

- [1] Zayas V, Mahin S and Constantinou MC (2017) Seismic Isolation Standard For Continued Functionality. *Technical Report: UCB/SEMM-2017/03*
- [2] ASCE 7 (2016) “*Minimum Design Loads and Associated Criteria for Buildings and Other Structures*”, American Society Of Civil Engineers
- [3] Fajfar, P. (2018). Analysis in seismic provisions for buildings: past, present and future: The fifth Prof. Nicholas Ambraseys lecture. *Bull Earthquake Eng* **16**, 2567–2608
- [4] Shao, B., Mahin, S.A., Zayas, V., (2019). Achieving targeted levels of reliability for low-rise seismically isolated structures. *Soil Dynamics and Earthquake Engineering* 125, 105744.
- [5] Kitayama, S and Constantinou MC (2019). Probabilistic seismic performance assessment of seismically isolated buildings designed by the procedures of ASCE/SEI 7 and other enhanced criteria. *Engineering Structures* **179**, 566–582.
- [6] Iervolino I, Spillatura A, Bazzurro P. (2018). Seismic Reliability of Code-Conforming Italian Buildings. *Journal of Earthquake Engineering*; **22**, 5-27.
- [7] Ragni L, Cardone D, Conte N, Dall’Asta A, Di Cesare A, Flora A, Leccese G, Micozzi F, Ponzo C. (2018) Modelling and seismic response analysis of Italian code-conforming base-isolated buildings. *Journal of Earthquake Engineering*; **22**, 198-230.
- [8] Nakazawa T., Kishiki S., Qu Z., Miyoshi A., Wada A. (2011). Fundamental Study on Probabilistic Evaluation of the Ultimate State of Base Isolated Structures, Proceedings, 8th International Conference on Urban Earthquake Engineering, Tokyo Institute of Technology, Tokyo, Japan
- [9] Dall’Asta A, Scozzese F, Ragni L, Tubaldi E. (2017) Effect of the damper property variability on the seismic reliability of linear systems equipped with viscous dampers. *Bull Earthq Eng*, 15:5025–53. doi:10.1007/s10518-017-0169-8
- [10] Scozzese F., Tubaldi E., Dall’Asta A. (2019). Seismic risk sensitivity of structures equipped with anti-seismic devices with uncertain properties. *Structural Safety*, Vol.77, 30-47
- [11] Dall’Asta A, Tubaldi E, Ragni L. (2016). Influence of the nonlinear behavior of viscous dampers on the seismic demand hazard of building frames. *Earthq Eng Struct Dyn*;45:149–69. doi:10.1002/eqe.2623
- [12] Gioiella L., Tubaldi E., Gara F., Dezi L., Dall’Asta A. (2018b). Modal properties and seismic behaviour of buildings equipped with external dissipative pinned rocking braced frames. *Engineering Structures*, Vol.172, 807-818 (ISSN:0141-0296).
- [13] Miyamoto HK, Gilani ASJ, Wada A, and Ariyaratana C (2011). Identifying the Collapse Hazard of Steel Special Moment-Frame Buildings with Viscous Dampers Using the FEMA P695 Methodology, *Earthquake Spectra*, Volume 27, No. 4, pages 1147–1168
- [14] EN15129. (2009) “*Antiseismic Devices*”, European Committee for Standardization, Brussels, Belgium.
- [15] Kikuchi M, Nakamura T, Aiken ID. (2010) Three-dimensional analysis for square seismic isolation bearings under large shear deformations and high axial loads. *Earthquake engineering and structural dynamics*; **39**:1513–1531.
- [16] Ishii K and Kikuchi M (2018) Improved numerical analysis for ultimate behavior of elastomeric seismic isolation bearings. *Earthquake engineering and structural dynamics*, **48**(1), 65-77.
- [17] Kikuchi M and Aiken ID (1997) An Analytical Hysteresis Model for Elastomeric Seismic Isolation Bearings, *Earthquake Engineering and Structural Dynamics*, **26**(2):215-231.
- [18] Kelly, J.M., (1997). *Earthquake-resistant design with rubber*. Springer London Ltd.
- [19] McKenna, F., (2011). OpenSees: A Framework for Earthquake Engineering Simulation. *Computing in Science Engineering* 13, 58–66.
- [20] Koh, C. G., and Kelly, J. M. (1986). “Effects of axial load on elastomeric bearings.” UCB/EERC-86/12, Earthquake Engrg. Res. Ctr., University of California, Berkeley, Calif.



- [21] Pant, D.R., Wijeyewickrema, A.C., ElGawady, M.A., 2013. Appropriate viscous damping for nonlinear time-history analysis of base-isolated reinforced concrete buildings: VISCOUS DAMPING FOR TIME-HISTORY ANALYSIS OF BASE-ISOLATED BUILDINGS. *Earthquake Engineering & Structural Dynamics* 42, 2321–2339. <https://doi.org/10.1002/eqe.2328>
- [22] Eurocode 8: Design of structures for earthquake resistance- Part 1: General rules, seismic actions and rules for buildings. European Committee for Standardization, Brussels, Belgium; 2004.
- [23] Bridgestone Corporation (2017) Seismic isolation product line-up.
- [24] Mitchell, D., Paultre, P., (1994). Ductility and overstrength in seismic design of reinforced concrete structures. *Can. J. Civ. Eng.* 21, 1049–1060. <https://doi.org/10.1139/194-109>
- [25] S.K. Au, J.L. Beck, Estimation of small failure probabilities in high dimensions by subset simulation, *Probabilistic Engineering Mechanics*. 16 (2001) 263–277. doi:10.1016/S0266-8920(01)00019-4.
- [26] S.K. Au, Y. Wang, *Engineering Risk Assessment with Subset Simulation*, 2014. doi:10.1002/9781118398050.
- [27] F. Jalayer, J.L. Beck, Effects of two alternative representations of ground-motion uncertainty on probabilistic seismic demand assessment of structures, *Earthquake Engineering and Structural Dynamics*. 37 (2008) 61–79. doi:10.1002/eqe.745.
- [28] C. Vetter, A.A. Taflanidis, Global sensitivity analysis for stochastic ground motion modeling in seismic-risk assessment, *Soil Dynamics and Earthquake Engineering*. 38 (2012) 128–143. <http://www.scopus.com/inward/record.url?eid=2-s2.0-84858618435&partnerID=40&md5=d4497f91e4f361a3fcf9992b594c79f6> (accessed 22 January 2018).
- [29] S.K. Au, J.L. Beck, Subset Simulation and its Application to Seismic Risk Based on Dynamic Analysis, *Journal of Engineering Mechanics*. 129 (2003) 901–917. doi:10.1061/(ASCE)0733-9399(2003)129:8(901).
- [30] S.L. Kramer, *Geotechnical Earthquake Engineering*, Prentice-Hall: Englewood Cliffs, NJ., 2003.
- [31] D.M. Boore, W.B. Joyner, Site amplifications for generic rock sites, *Bulletin of the Seismological Society of America*. 87 (1997) 327–341. <http://www.bssaonline.org/content/87/2/327.short> (accessed 22 January 2018).
- [32] G.M. Atkinson, W. Silva, Stochastic modeling of California ground motions, *Bulletin of the Seismological Society of America*. 90 (2000) 255–274. doi:10.1785/0119990064.
- [33] D.M. Boore, Simulation of Ground Motion Using the Stochastic Method, in: *Seismic Motion, Lithospheric Structures, Earthquake and Volcanic Sources: The Keiiti Aki Volume*, Birkhäuser Basel, Basel, 2003: pp. 635–676. doi:10.1007/978-3-0348-8010-7\_10.
- [34] Hong, H. P., & Liu, T. J. (2014). Assessment of coherency for bidirectional horizontal ground motions and its application for simulating records at multiple stations. *Bulletin of the Seismological Society of America*, 104(5), 2491-2502.
- [35] Baker, J. W., & Cornell, C. A. (2006). Correlation of response spectral values for multicomponent ground motions. *Bulletin of the seismological Society of America*, 96(1), 215-227.
- [36] Mizukoshi, K., Yasaka, A., Iizuka, M., Takabayashi, K., (1992). Failure test of laminated rubber bearings with various shapes. *Earthquake Engineering, Tenth World Conference*. Balkema, Rotterdam.
- [37] Nishi, T., Suzuki, S., Aoki, M., Sawada, T., Fukuda, S., 2019. International investigation of shear displacement capacity of various elastomeric seismic-protection isolators for buildings. *J Rubber Res* 22, 33–41. <https://doi.org/10.1007/s42464-019-00006-x>
- [38] European Committee for Standardization. EN 15129:2010 - Antiseismic devices. 2010.
- [39] ASCE 41-13: *Seismic Evaluation and Retrofit Rehabilitation of Existing Buildings* 2014. doi:10.1061/9780784412855.
- [40] Kikuchi, M., Black, C.J., Aiken, I.D., 2008. On the response of yielding seismically isolated structures. *Earthquake Engng Struct. Dyn.* 37, 659–679. <https://doi.org/10.1002/eqe.777>